MODELS OF SPACE ENERGETICS OF COUPLED STRUCTURAL SYSTEMS AT AN ARBITRARY ANGLE

Edmilson R. O. Santos

José R. F. Arruda

José M. C. Dos Santos

Universidade Estadual de Campinas
Faculdade de Engenharia Mecânica
Departamento de Mecânica Computacional, FEM, C.P. 6122, Campinas - SP CEP 13083-970
[oliveira, arruda, zema]@fem.unicamp.br

Abstract. *Energy Finite Element Method (EFEM) is based on approximation solution of partial differential equations resulting of energy balance and joint relationship for various structural configurations and wave types. The joint relationships are used to describe the energy exchange among various systems. EFEM can be expressed in a standard Finite Element (FE) approach, similar to heat conduction problems. Spectral Element Method (SEM) is an approach similar to FE based on a mode propagation superposition. Differently of FE methods in which a differential equation is solved as an approximation, SEM represents the exact solution of the wave equation. Also is presented an other approach, which is being called ESEM. The spectral formulation is applied for differential equation of energy. ESEM has element dynamic stiffness computed from the analytical solution of the differential equation energy. In this paper this methods are used to predict vibration response of dynamic system at high frequencies. By using longitudinal and transversal wave energy finite element for different joints couplings, some simulated cases are analyzed and compared with the solutions obtained by SEM. Also, experimental tests results from a bar and a T-shape joint beam are presented and compared with the simulated ones.*

Keywords*: Spectral Element Method, Energy Finite Element Method, Energy Spectral Element Method, high frequencies, beam, joint matrix.*

1. Introduction

Acoustical and vibrational energy are normally borne by waveguides such as rods and beams. Many structural engineering problems involve this type of components, which produce a restricted vibration and noise transmission path. However, a review in the literature shows that approaches to low-frequency range are extensively used and there is still a need for predictive tools able to solve energy propagation mechanism for rods and beams in the medium and high-frequency domain. Different methods are on development to provide predictive tools adequate to these domains. Classical methods, like finite element, boundary element, etc., have inherent characteristics that make its use inadequate in the high modal density range. Therefore, medium and high-frequency behavior of complex structures is still an active subject of investigation. In this work two of these methods are explored: the Spectral Element Method (SEM) and the Energy Finite Element Method (EFEM). The SEM is based upon the analytical solution of wave partial differential equations in the frequency domain. The EFEM is an approximate solution of the energy differential equations, expressed as a standard FE method. Similar works have been published in these directions (Cho, 1993; Doyle, 1989 and Moens, 2001), but there are some issues which have not been addressed previously and will be discussed in this paper. Also, a new method called Energy Spectral Element Method (ESEM) is proposed and some simulated results are presented and compared with the other methods.

2. Review of Spectral Element and Energy Finite Element Methods

Complete SEM formulation for elementary rod and beam (Bernoulli-Euler and Timoshenko) can be found in Doyle (1989). The examples treated in this paper were formulated using the elementary rod element, the Bernoulli-Euler beam element and the spectral frame element, which consists of a bar (traction) and a beam (flexure) element combination. For all examples, only vibrations in the plane that contains the waveguides were considered. Therefore, from the analytical responses obtained by SEM, the analytical energy density was calculated for each wave type (Cho, 1989). The dynamic stiffness relation to the spectral element for rods is established via *dynamic shape functions*, which are shape functions between element nodes, but instead of being simple polynomials, they are the exact displacement distributions. The longitudinal displacement for a rod is given by:

$$\hat{u}(x) = \mathbf{A}e^{-ikx} + \mathbf{B}e^{-ik(L-x)} \tag{1}$$

where k is the wave number, L is the element length and **A**, **B** are constants determined from the boundary conditions. The displacement end conditions for a two nodes element are

$$\hat{u}(0) \equiv \hat{u}_1 = \mathbf{A} + \mathbf{B}\mathbf{e}^{-ikL}, \qquad \hat{u}(L) \equiv \hat{u}_2 = \mathbf{A}\mathbf{e}^{-ikL} + \mathbf{B} \tag{2}$$

where u_1 and u_2 are the nodal displacements. By solving for **A**, **B** in terms of nodal displacements, the longitudinal displacement at an arbitrary point in a finite rod is

$$\hat{u}(x) = \hat{g}_1(x)\hat{u}_1 + \hat{g}_2(x)\hat{u}_2 \tag{3}$$

where $\hat{g}_1(x) = \left(\mathbf{e}^{-ikx} - \mathbf{e}^{-ik(2L-x)}\right)/\left(1-\mathbf{e}^{-i2kL}\right)$, $\hat{g}_2(x) = \left(-\mathbf{e}^{-ik(L+x)} + \mathbf{e}^{-ik(2L-x)}\right)/\left(1-\mathbf{e}^{-i2kL}\right)$ are the frequency-dependent rod shape function. The member force at an arbitrary point in a finite rod can be obtained as

$$\hat{F}(x) = \hat{E}A\left[\hat{g}_1'(x)\hat{u}_1 + \hat{g}_2'(x)\hat{u}_2\right] \tag{4}$$

and the dynamic stiffness for two nodes element can be written in a matrix form as

$$\begin{Bmatrix} \hat{F}_1 \\ \hat{F}_2 \end{Bmatrix} = \frac{\hat{E}A}{L}\frac{ikL}{\left(1-\mathbf{e}^{-i2kL}\right)}\begin{bmatrix} 1+\mathbf{e}^{-i2kL} & -2\mathbf{e}^{-i2kL} \\ -2\mathbf{e}^{-i2kL} & 1+\mathbf{e}^{-i2kL} \end{bmatrix}\begin{Bmatrix} \hat{u}_1 \\ \hat{u}_2 \end{Bmatrix} \tag{5}$$

Governing energy equations for the propagation of longitudinal waves in a steady state, harmonically excited rod with small structural loss factor were obtained by Wohlever (1988):

$$\frac{c_g^2}{\eta\omega}\frac{d^2\langle e\rangle}{dx^2} - \eta\omega\langle e\rangle = 0 \tag{6}$$

where, $\langle e\rangle$ is the time-average energy density, η is the structural loss factor, ω is the circular frequency, and c_g is the group velocity. The general solution to equation (6) is given by:

$$\langle e\rangle = G_1\mathbf{e}^{\left(\frac{\eta\omega}{c_g}x\right)} + G_2\mathbf{e}^{\left(-\frac{\eta\omega}{c_g}x\right)} \tag{7}$$

where, G_1 and G_2 are constants determined by applying the boundary conditions. Equation (7) can be used to predict the frequency-averaged energy per length unit and energy power flow distributions in a finite structure at high frequencies [5], and this approach is called Energy Flow Analysis (EFA).

Equation (6) can also be solved as an FE approximation called EFEM (Cho,1989), which allows predicting the spatial variation of energy throughout the system. The element matrix form for ith element can be written as:

$$\left[\left[E^{(e)}\right]_i^j + \left[J\right]_i^j\right]\left\{e^{(e)}\right\}_i^j = \left\{F^{(e)}\right\}_i^j \tag{8}$$

where superscript (e) indicates element-based quantities, subscript i and j indicates the ith and jth element, $\{e^{(e)}\}_j^i$ the vector of nodal values for the time and space averaged energy density, $[E^{(e)}]_j^i$ is the dynamic system matrix, $[J]_j^i$ is the joint matrix and $\{F^{(e)}\}_j^i$ the vector of nodal inter-element power flow. Since the energy density is discontinuous at joint, an especial global assembly procedure is used to assemble the element matrix, and the joint matrix is obtained using energy flow coupling relationships (transmission and reflection coefficients) for different structural joints.

3. Energy spectral element method

"*The only way to efficiently handle wave propagation problems in structures with complicated boundaries and discontinuities is to develop a matrix methodology for use on a computer*", Doyle (1989). Based on this statement a new approach is proposed, which is obtained by applying the spectral formulation concept to the EFA solution. This is named Energy Spectral Element Method (ESEM), and it has the dynamic relation for rods computed via dynamic shape functions, which are the exact energy density distributions from the analytical solution of the energy differential equation (eq. 6). The spatial and frequency-averaged energy per length longitudinal energy density for a rod is given by

the eq. (7). By applying, either specified energy density or energy power flow boundary conditions to an uniform waveguide of finite length L, it ends up with a dynamic system for two nodes rod element given by:

$$\begin{Bmatrix} \langle q \rangle_1 \\ \langle q \rangle_2 \end{Bmatrix} = -\frac{c_{gi}^2}{\eta\omega} \begin{bmatrix} \psi & -\psi \\ \psi e^{\psi L} & -\psi e^{-\psi L} \end{bmatrix} \begin{bmatrix} 1 & 1 \\ \psi e^{\psi L} & \psi e^{-\psi L} \end{bmatrix}^{-1} \begin{Bmatrix} \langle e \rangle_1 \\ \langle e \rangle_2 \end{Bmatrix} = [k_L] \{\langle e \rangle\} \tag{9}$$

where k_L is the frequency dependent dynamic element matrix for rod, $\langle q \rangle$ is energy power flow vector, $\langle e \rangle$ is energy density vector and $\psi = \eta\omega/c_g$.

4. Comparing SEM, EFEM and ESEM

Two cases were simulated using SEM, EFEM, and ESEM methods with the following configuration: two free-free beams coupled at arbitrary angles and three free-free beams in T-shape. The used frequency range criteria to EFEM and ESEM validity was a mode count of at least 3 and a modal overlap factor (MOF) greater than 0.5(Cho, 1989; Lyon, 1995; and Plunt *et al* , 1993). Figure 1 shows the approximate mode count and MOF versus the central frequency band to rods and beams, A and B.

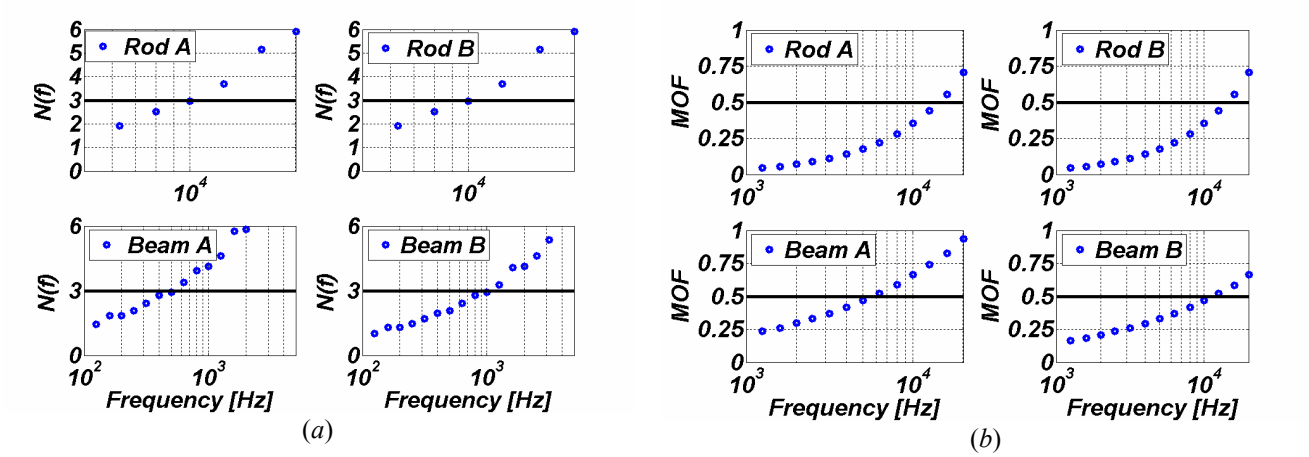

Figure 1. Rods and beams, A and B frequency range validity to EFEM and ESEM: (*a*) N(f) and (*b*) MOF.

Figure 2 shows the configuration for two beams connected at an arbitrary angle and excited at the left end by longitudinal and flexural harmonic forces. The structure is made of aluminum with parameters and dimensions given by: lengths L_A= L_B=3 m; cross sections areas A_A=A_B=16e-10 m^2; density ρ =2700 kg/m^3; loss factor η=0.03; and Young's modulus E=71 GPa. The frequency-averaged longitudinal and flexural energy densities and energy flow were calculated for different angles ranging from 0° to 90°, and for a 1/12-octave band with center frequencies of 6.3 and 12.5 kHz.

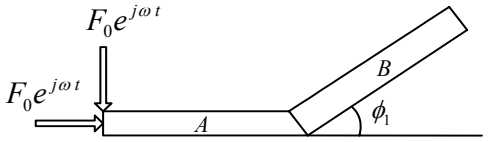

Figure 2. Two coupled beams at arbitrary angle with longitudinal and flexural excitations

Simulated frequency-averaged longitudinal and flexural total energy densities and power flows were calculated using ESEM, SEM and EFEM. For each excitation, there will be longitudinal and flexural wave couplings, and the joint matrix in EFEM becomes more elaborate (Santos, 2005). To clarify the results, the terms related to each wave type were calculated and analyzed separately. The longitudinal and flexural total energy densities are written as $\langle e \rangle_{LAB} = \langle e \rangle_{LLAB} + \langle e \rangle_{LFAB}$ and $\langle e \rangle_{FAB} = \langle e \rangle_{FFAB} + \langle e \rangle_{FLAB}$, respectively, where: $\langle e \rangle_{LLAB}$ is the longitudinal energy due longitudinal wave from beam A to B; $\langle e \rangle_{LFAB}$ is the longitudinal energy due flexural wave from A to B; $\langle e \rangle_{FLAB}$ is the flexural energy due longitudinal wave from A to B; and $\langle e \rangle_{FFAB}$ is the flexural energy due flexural wave from A to B. Same pattern is also used to present the energy power flow results.

Although the problem has been solved to an angle range between 0° to 90°, only a typical result for 60° will be presented here. The results for the terms and total energy density and power flow can be seen in figures 3 and 4, respectively. Almost all plots are in good agreement among the three methods, except for the plots $\langle e \rangle_{FLAB}$ and $\langle e \rangle_{LFAB}$ which present some differences between SEM and the other methods at center frequency band 6.3 kHz. However, there

is no appreciable effect on the total energy density. Similar behavior can be observed with energy power flow plots. This difference seems to be due the low mode count and MOF for the rod and/or beam at this frequency band. The results of energy density and power flow obtained by ESEM and shown in figures 3 and 4, respectively, are re-plotted in figures 5 and 6 to illustrate a new and more intuitive graphical presentation.

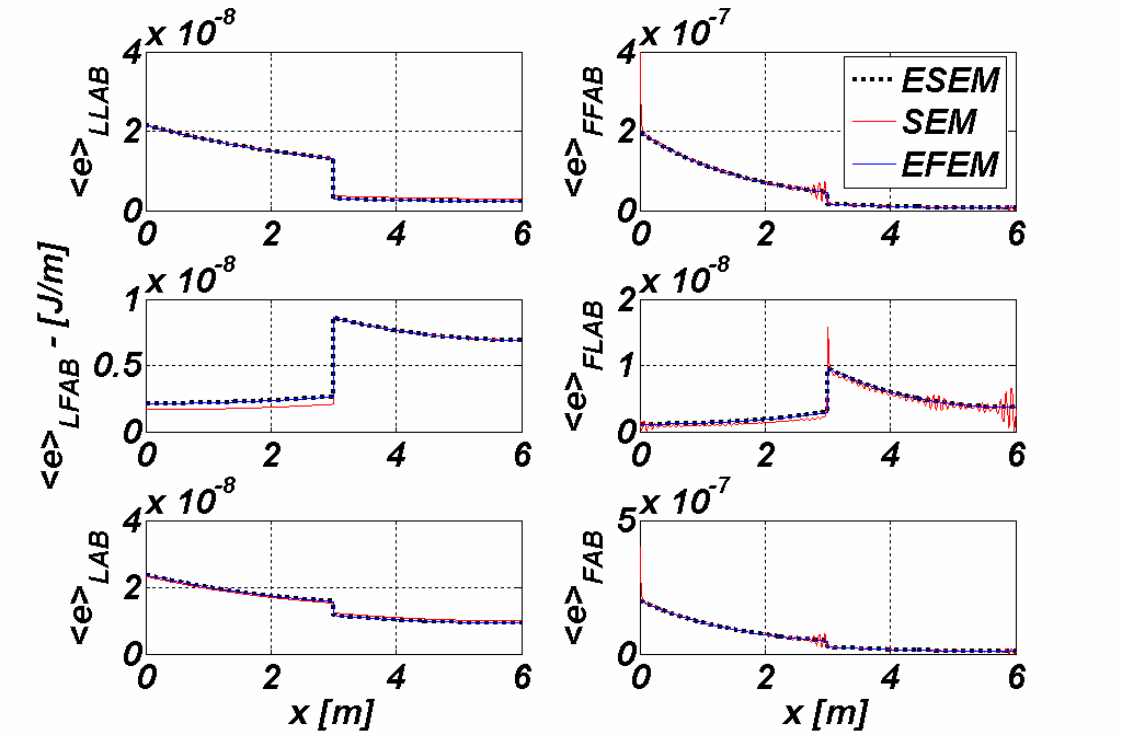

(a) center frequency band 6.3kHz

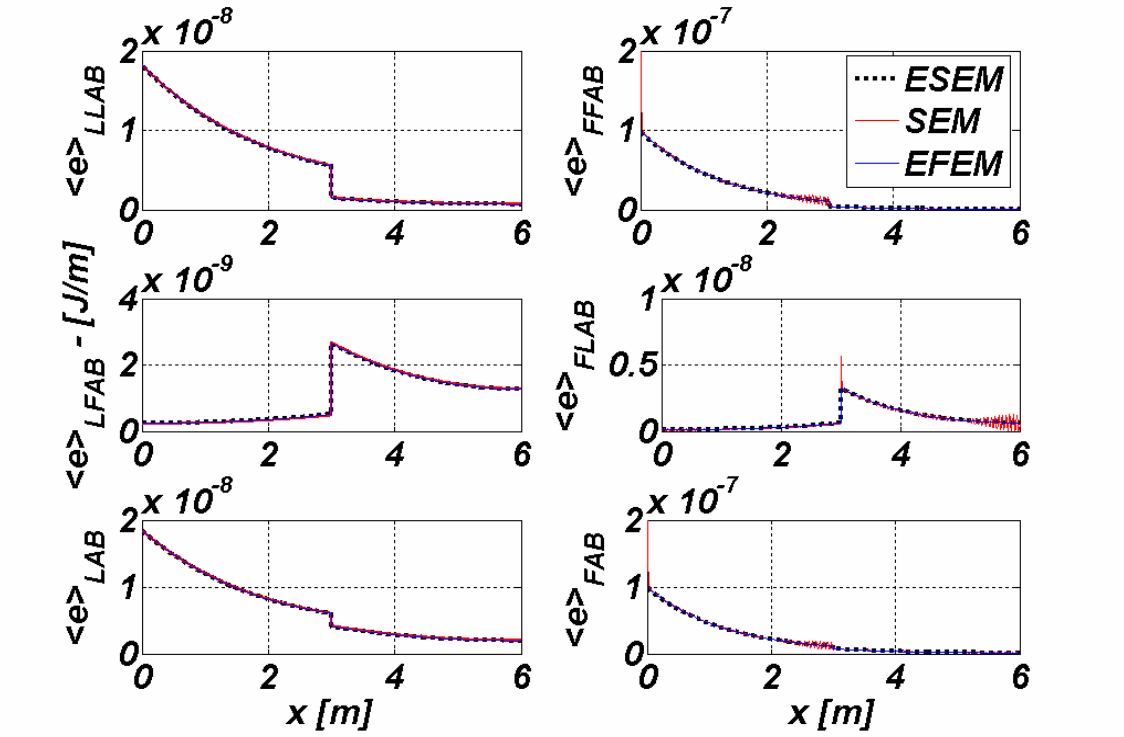

(b) center frequency band 12.5kHz

Figure 3. Coupled beams with 60° - energy density by ESEM, SEM and EFEM.

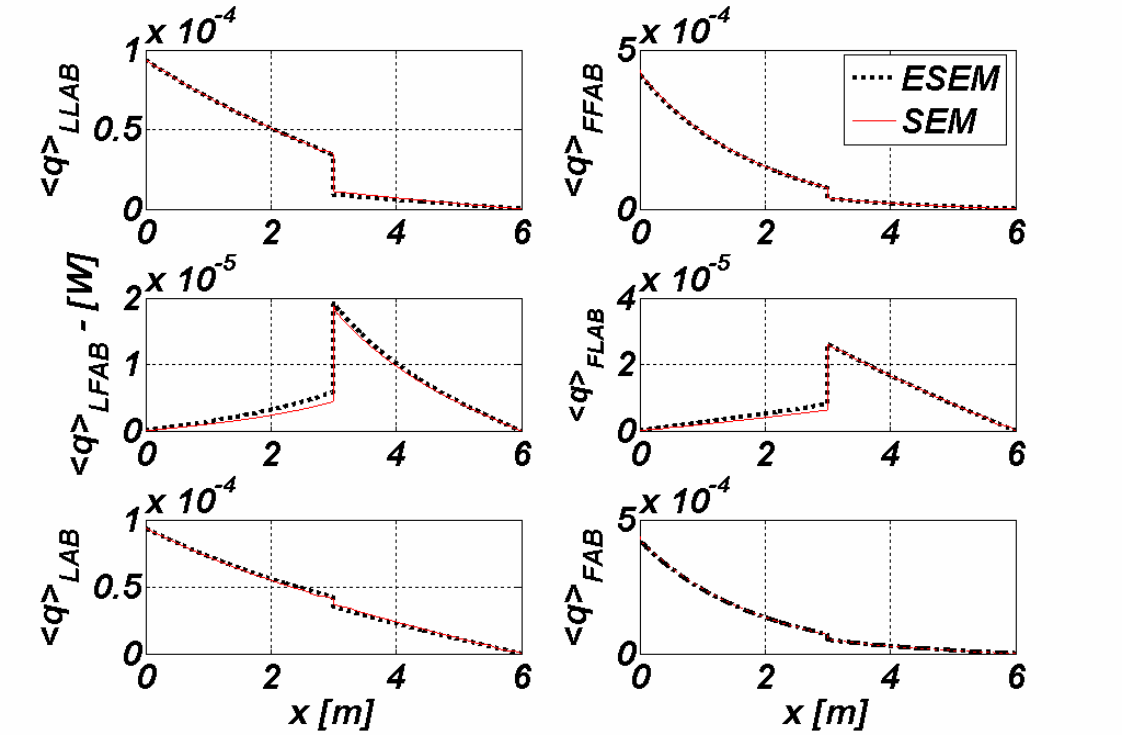

(a) center frequency band 6.3kHz

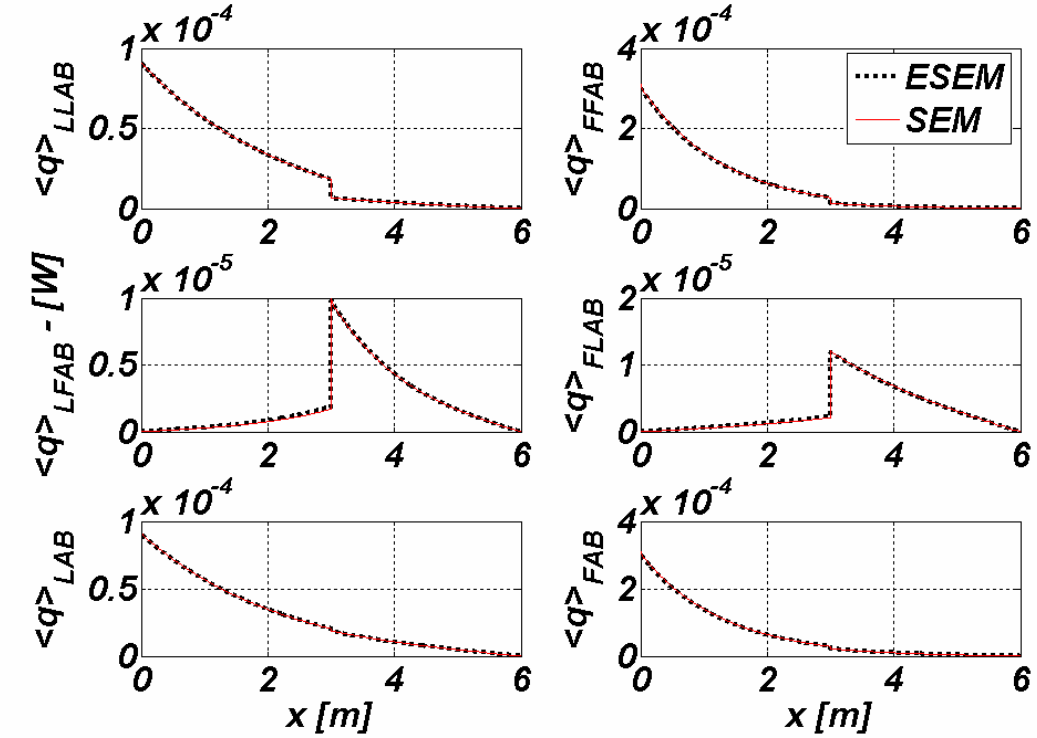

(b) center frequency band 12.5kHz

Figure 4. Coupled beams at 60° angle – energy power flow by ESEM and SEM.

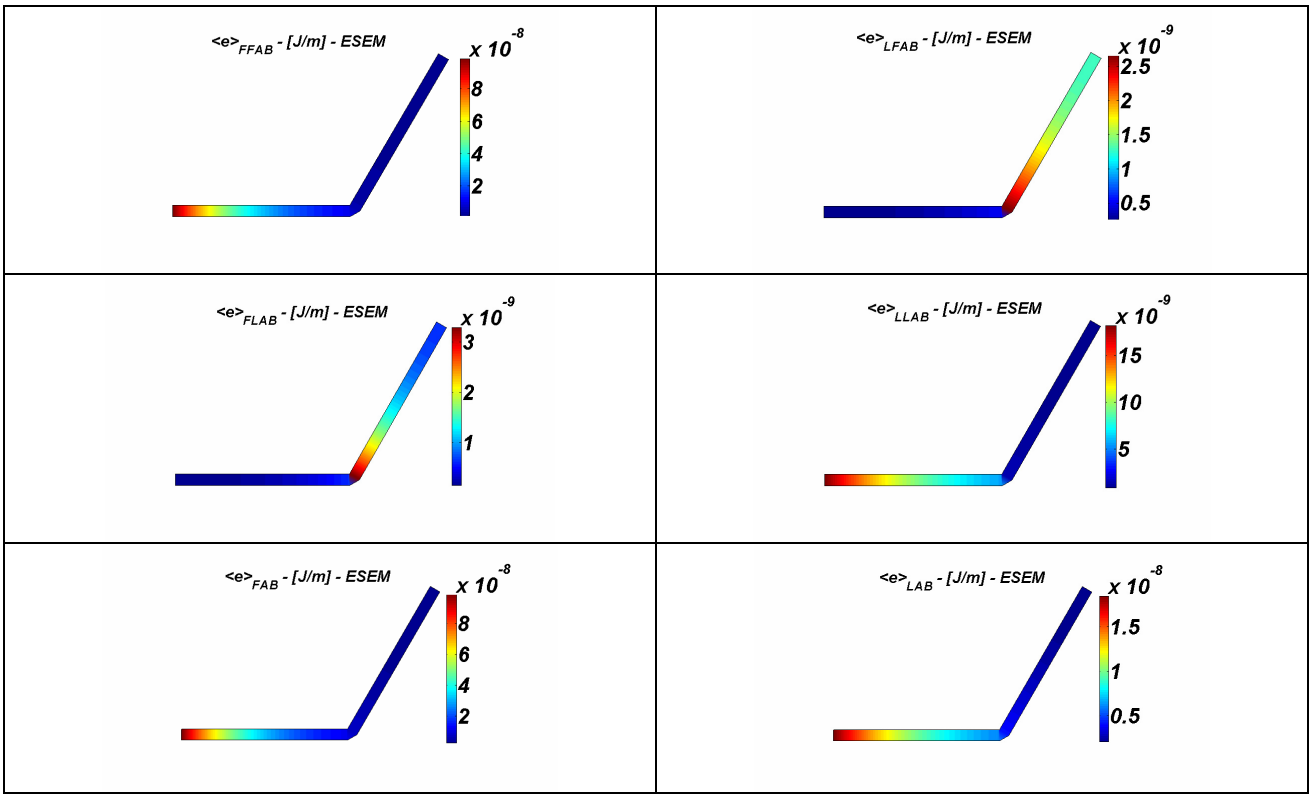

Figure 5. Coupled beams at 60° angle - new graphic presentation energy density by ESEM.

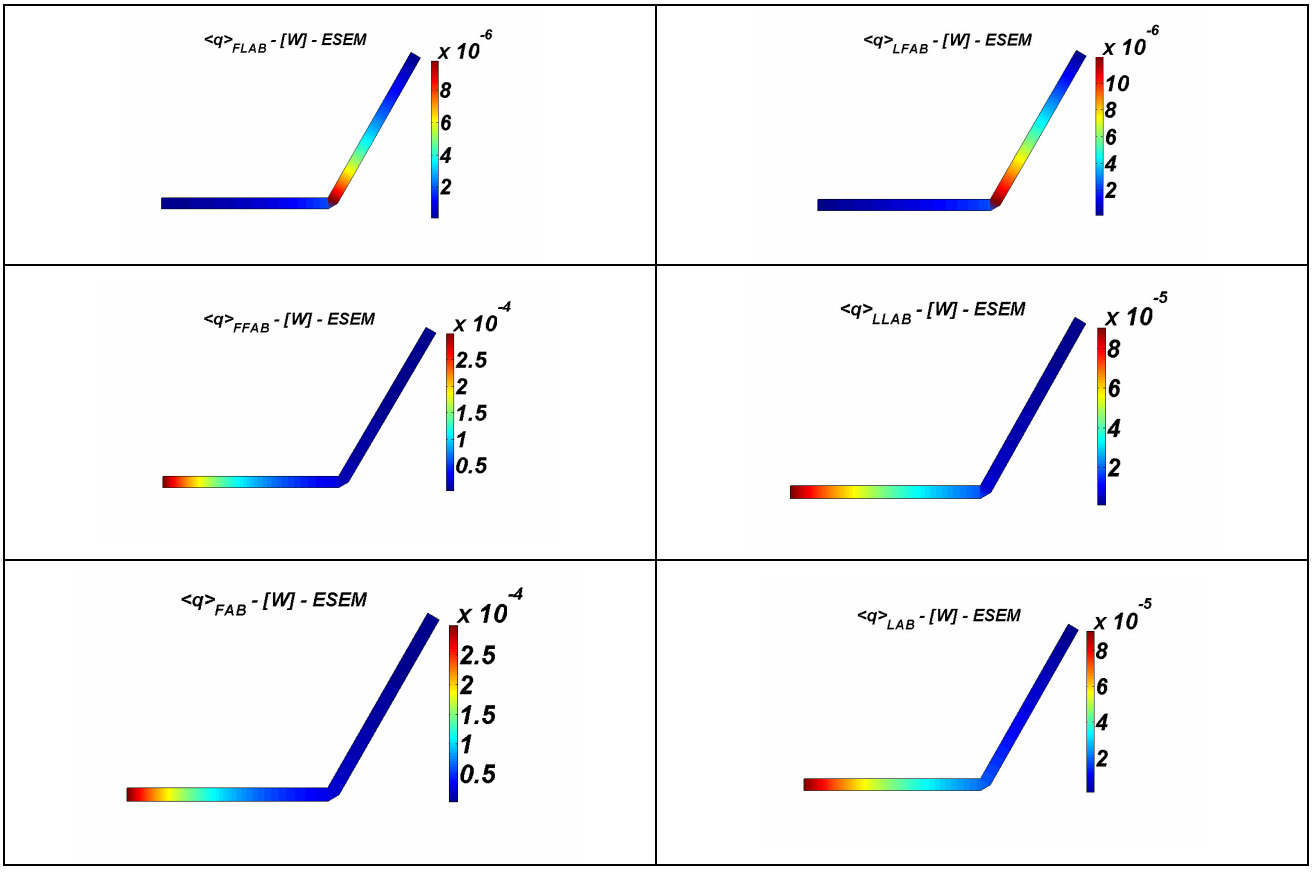

Figure 6. Coupled beams at 60° angle - energy power flow by ESEM

Figure 7*a* shows the T-beam aspect excited by longitudinal and flexural harmonic forces. It consists of three beams A, B and C connected at the joint with angles 0° and 90°. The T-beam is an actual structure used in a Round-Robin research (Hambric, 1995), where it is intended to validate the simulated model with experimental results. The T-beam is made of Lexan, continuous at the joints and, its properties are: density, ρ =1280 kg/m^3; Poisson rate, ν=0.25, cross section, A=1.7118000e-3 m^2, inertia moment, I =1.4334755e-7 m^4, loss factor, η=0.03 and Young's modulus, E= 2.62 GPa.

To reproduce free-free conditions in the test, the T-beam was suspended by nylon fish lines at three points and excited in the longitudinal and flexural directions at the end of branch A (Figure 7*b*). The excitation was applied using an electromechanical shaker, which is driven by a periodic chirp signal in the frequency range of DC-8 kHz with intervals of 0.5 Hz. A signal generator and a data acquisition system (HP 3314A) were used. The shaker was connected to a stinger, which was connected to a force transducer PCB model 208A02. The acceleration frequency response functions (FRF) at 111 points along the structure were measured using three PCB 353B68 accelerometers. The data acquisition was conducted by LMS CADA-X 3.8v software.

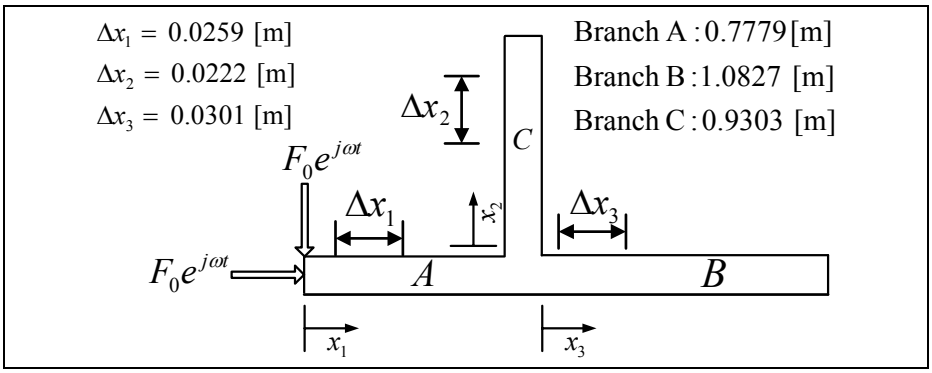

(a)

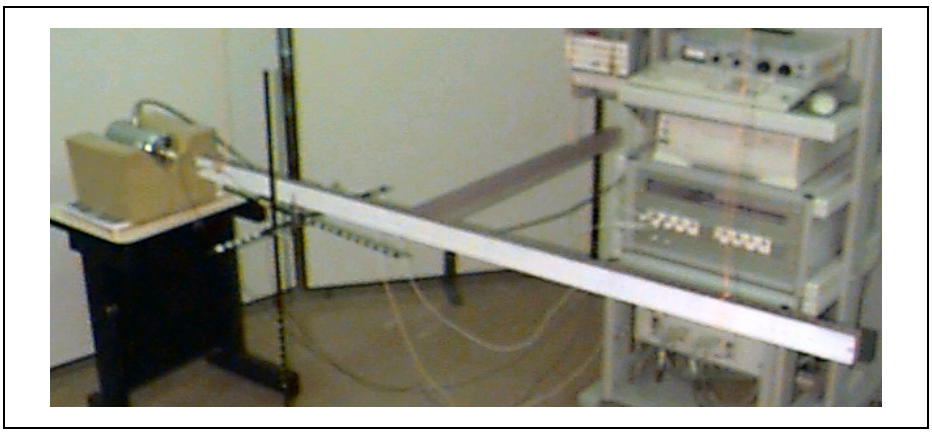

(b)

Figure 7. T-beam: (a) configuration and dimensions (b) experimental setup.

The simulated terms and the total energy density and power flow for the T-beam systems at central frequency of 6.3 kHz are shown in figures 8 and 9 respectively. As revealed before in the case of coupled beams at arbitrary angle, some plots of cross transmission between flexural and longitudinal waves are in disagreement. For example, in figure 8a $\langle e \rangle_{FLAB}$ between branch AC and in figure 8b $\langle e \rangle_{LFAB}$ between branch AB presents disagreement between SEM and other plots. Since its contributions are smaller then the other terms, there is no significant effect on the total longitudinal and flexural energy densities ($\langle e \rangle_{LAB}$ and $\langle e \rangle_{FAB}$). Similar behavior can be observed to the energy power flow plots.

Figures 10 and 11 shows the energy densities simulated by EFEM and ESEM, and interpolated with experimental data by SEM, for 1/12-octave band with center frequency of 6.3 and 4.0 kHz, respectively. The experimental longitudinal and flexural energy density was estimated using an interpolation SEM procedure. It consists in to integrate twice the measured acceleration FRF's to obtain the displacement FRF's. Then, they are introduced in the spectral wave equation solution to obtain the coefficients, which can be used to interpolate a spatial SEM solution and calculate the longitudinal and flexural energy density. Due the ill-conditioning generated by evanescent wave component coefficients, they were neglected in all calculation of energy densities. The $\langle e \rangle_{LAB}$ simulated by EFEM and ESEM were obtained by using the input power calculated from the experimental acceleration FRF at the driving point.

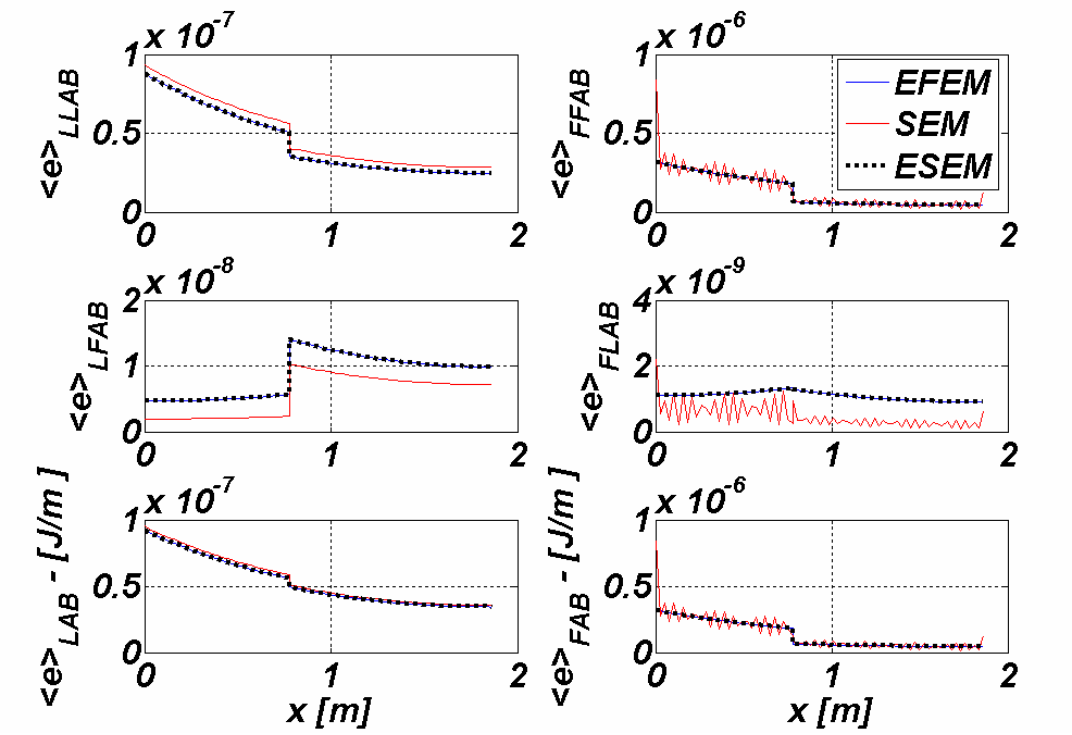

(a) branch AB, ϕ =0°

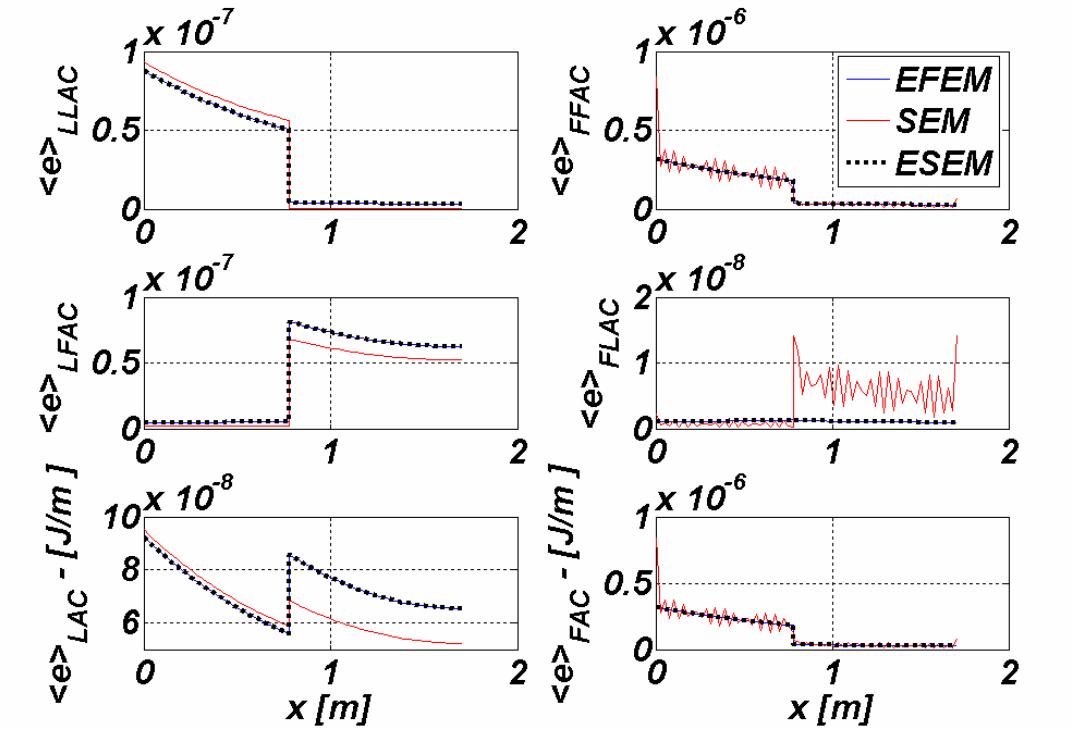

(b) branch AC, ϕ = 90°

Figure 8. T-Beam simulated energy density by EFEM, SEM and ESEM at center frequency band 6.3 kHz.

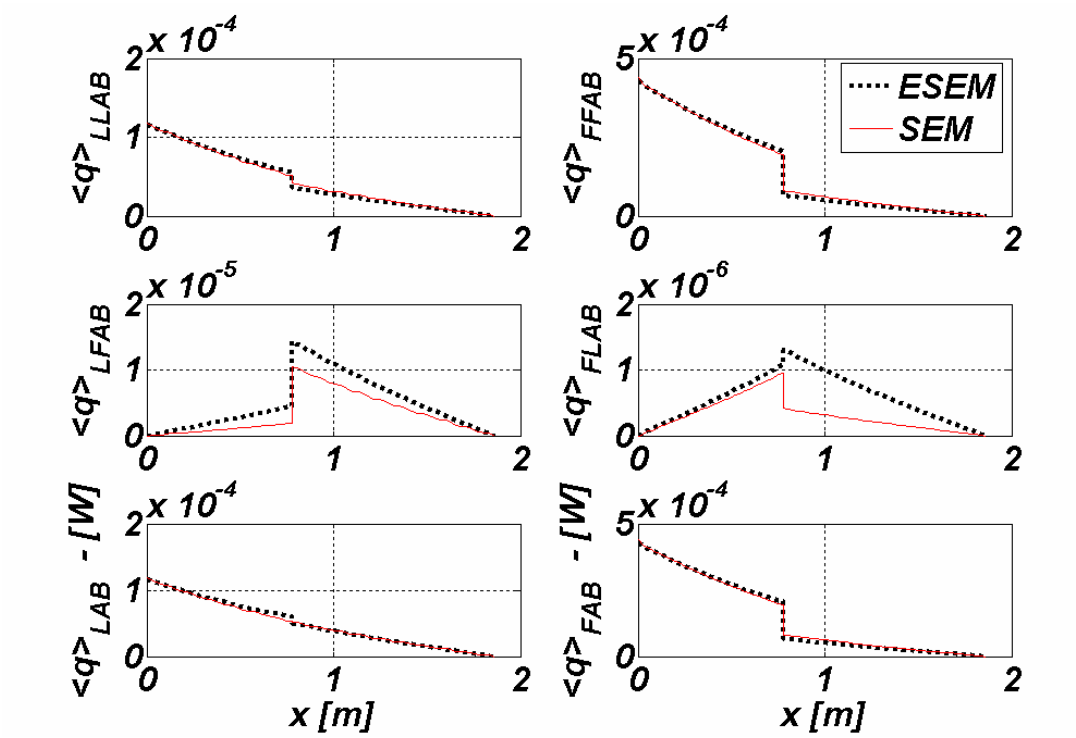

(a) branch AB, ϕ =0°

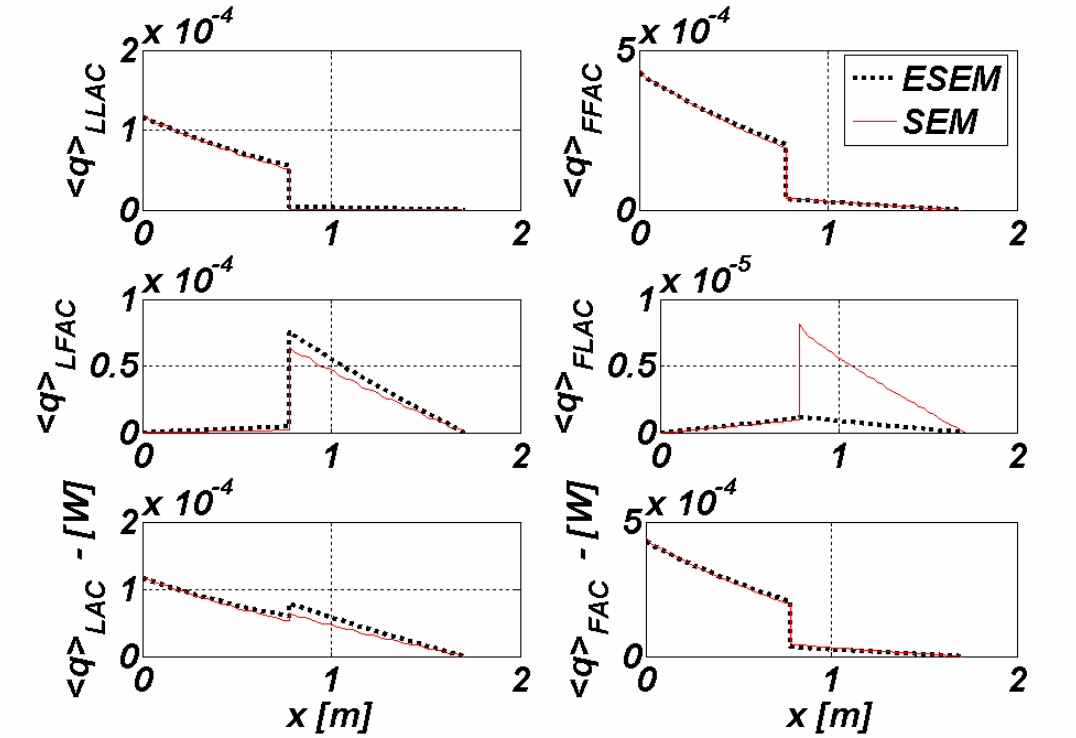

(b) branch AC, ϕ = 90°

Figure 9. T-Beam simulated energy power flow by ESEM and SEM at center frequency band 6.3 kHz.

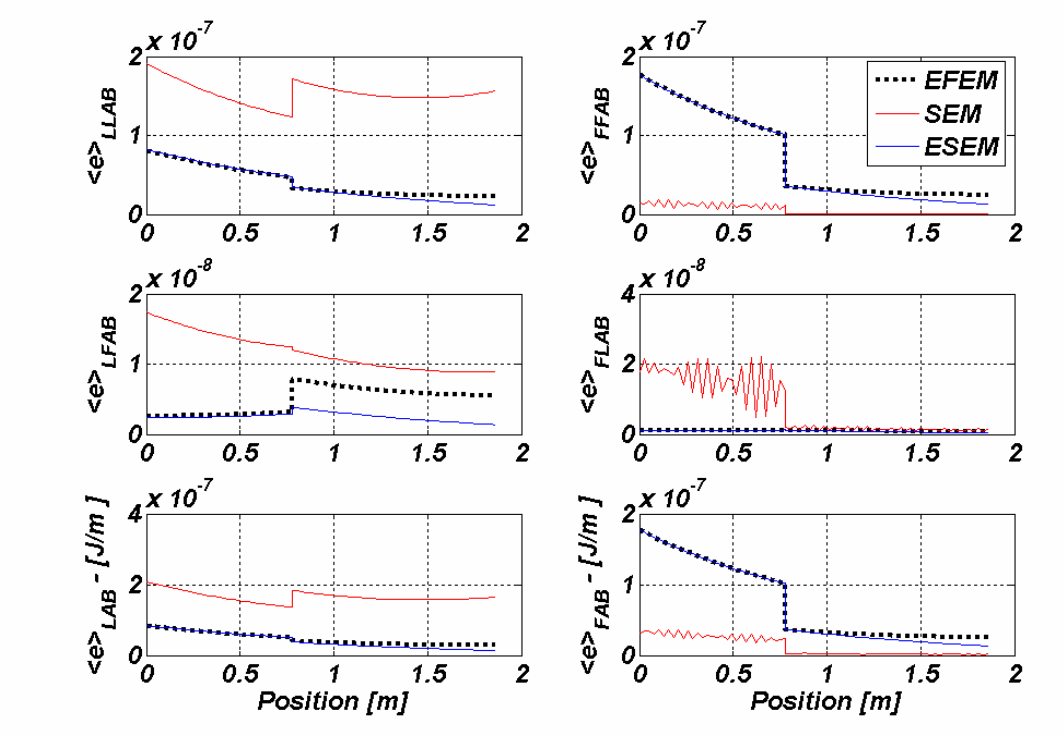

(a) branch AB, ϕ =0°

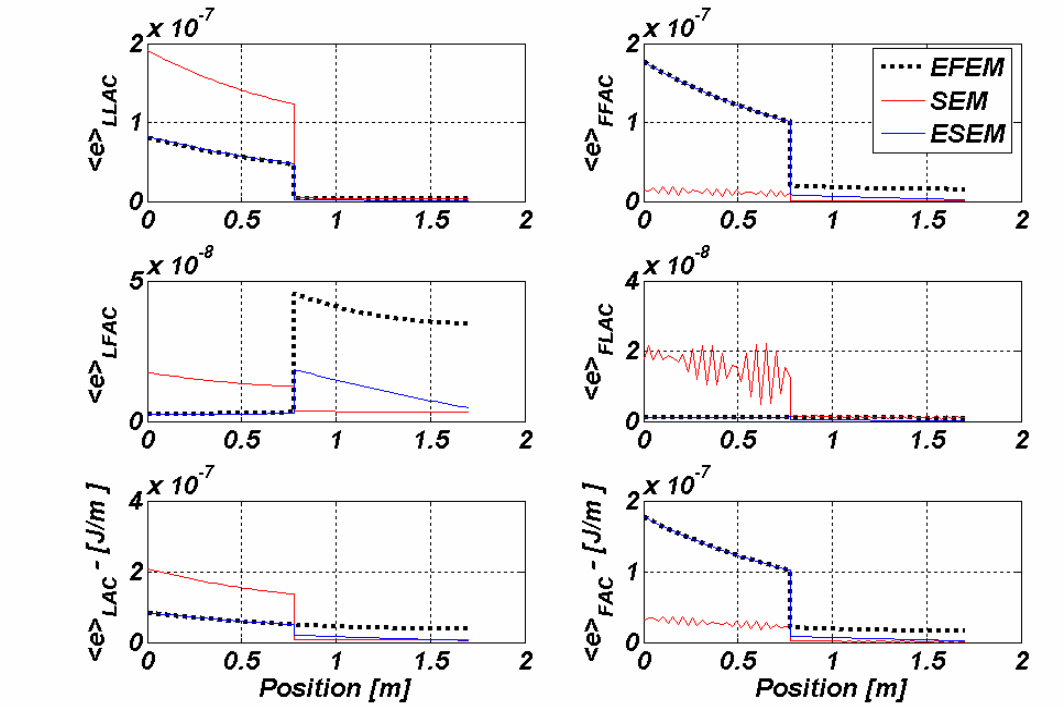

(b) branch AC, ϕ = 90°

Figure 10. T-Beam energy densities by SEM interpolated with experimental data and simulated EFEM and ESEM at center frequency band 6.3 kHz.

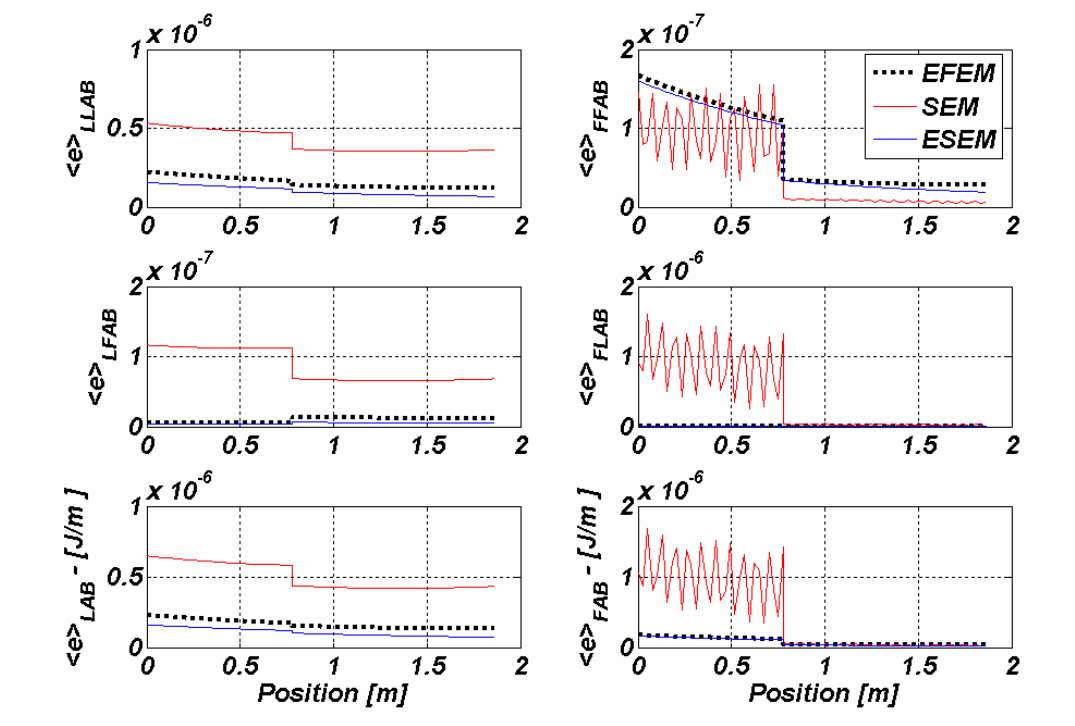

(a) branch AB, ϕ =0°

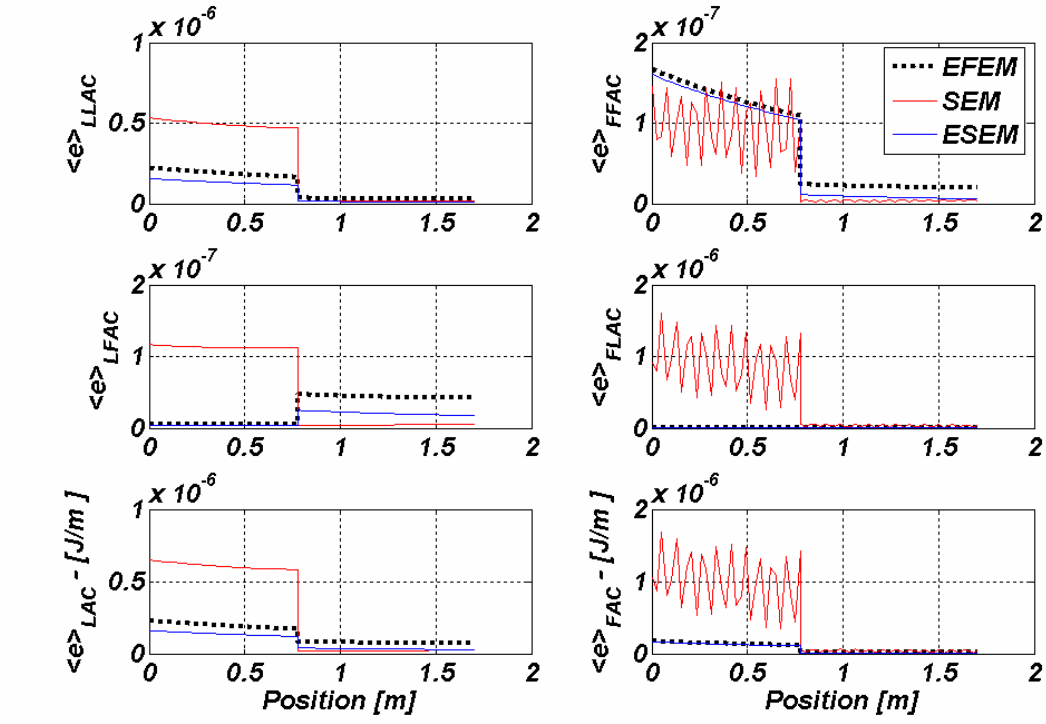

(b) branch AC, ϕ = 90°

Figure 11. T-Beam energy densities by SEM interpolated with experimental data and simulated EFEM and ESEM at center frequency band 4.0 kHz.

As can be seen the results from SEM interpolated with experimental data and simulated by EFEM and ESEM presents many disagreements. Some of them are related with differences in amplitude only, but keeping a consistent spatial behavior relative to raise or lower the energy density levels. For example, at center frequency band 4.0 kHz (figure 11) the longitudinal and flexural total energy densities ($\langle e \rangle_{LAB}$ and $\langle e \rangle_{FAB}$) to the branch AB and AC presents

the same behavior, but with different amplitudes. Nevertheless, at center frequency band 6.3 kHz (figure 10) only the flexural total energy density ($<e>_{FAB}$) to the branch AB and AC presents such behavior, while longitudinal total energy density ($<e>_{LAB}$) are in total disagree.

5. CONCLUSIONS

A new method named Energy Spectral Element Method (ESEM) is proposed. Different cases were simulated comparing SEM, ESEM and EFEM to the following configurations: free-free beams coupled at arbitrary angle and; free-free beams coupled at T-shape. Experimental test to the configuration coupled at T-shape was made. Simulated and, experimental when applicable, were compared and discussed. A more intuitive graphical presentation to the energy density and power flow was presented. SEM was used as a reference, since it is based upon an exact solution of the wave equation. EFEM is suitable for higher frequencies, as it predicts an average behavior in a statistical sense, with mechanical energy densities as the primary variables. EFEM produces good results when the analyses were performed at higher frequencies provided the loss factor was not too small. Longitudinal and flexural energy density and power flow was interpolated by SEM with experimental data and simulated by EFEM and ESEM for a T-shape beam. The results were compared and although it presents same tendency in terms of global behavior there are still many disagreements in terms of amplitude. However, it should be emphasized that these are preliminary results and more investigation is under way.

6. Acknowledgements

The authors are grateful to the government research funding agencies FAPESP, CNPq and CAPES for the financial support.

7. References

Cho, P. E., “Energy Flow Analysis of Coupled Structures”, PhD thesis, Purdue University, Lafayette, USA, (1993).

Doyle, J. F., “Wave Propagation in Structures”, Prentice-Hall, New York, USA, (1989).

Hambric, S. A., “Comparison of Finite Element Predictions and Experimental Measurements of Structure-Borne Powers In a T-Shaped Beam”, Proceedings of Inter-noise 95, Newport-Beach, CA, USA, July,10-12, (1995).

Lyon, R. H., “Theory and Application of Statistical Energy Analysis”, M.I.T. Press, Second Edition, (1995).

Moens, I., “On the Use and Validity of The Energy Finite Element Method For High Frequency Vibrations”, PhD thesis, Leuven Catholic University, Belgium, 2001.

Plunt, J., Fredo, C. and Sanderson, M., “On the Use and Misuse of Statistical Energy Analysis for Vehicle Noise Control”, Proceedings of the SAE Noise and Vibration Conference, p. 319-328, (1993).

Santos, E.O., Donadon, L.V., Arruda, J.R.F., Dos Santos, J. M. C., “Analysis of Coupled Structural Systems using Energy Finite Elements and Spectral Elements ” , 12th International Congress on Sound and Vibration, Lisbon, 11-14 July (2005).

Wohlever, J. C., “Vibration Power Flow Analysis of Rods and Beams”, PhD thesis, Purdue University, Lafayette, USA, (1988).

8. Responsibility notice

The authors are the only responsible for the printed material included in this paper.